

## Mechanical and Biomechanical Characterization of a Polyurethane Nucleus Replacement Device Injected and Cured In Situ Within a Balloon

Anthony Tsantrizos, Nathaniel R. Ordway, Khin Myint, Erik Martz and Hansen A. Yuan

*Int J Spine Surg* 2008, 2 (1) 28-39

doi: <https://doi.org/10.1016/SASJ-2007-0113-RR>

<https://www.ijssurgery.com/content/2/1/28>

This information is current as of May 16, 2025.

---

**Email Alerts** Receive free email-alerts when new articles cite this article. Sign up at:  
<http://ijssurgery.com/alerts>

## Mechanical and Biomechanical Characterization of a Polyurethane Nucleus Replacement Device Injected and Cured In Situ Within a Balloon

*Anthony Tsantrizos, MSc, PhD, Nathaniel R. Ordway, MS, PE, Khin Myint, Erik Martz, MSc, and Hansen A. Yuan, MD*

### ABSTRACT

#### Background

The DASCOR device has recently been introduced as an innovative nucleus replacement alternative for the treatment of low-back pain caused by degenerative intervertebral disc disease. The purpose of this study was to characterize, through a series of preclinical mechanical bench and biomechanical tests, the effectiveness of this device.

#### Methods

A number of samples were created using similar preparation methods in order to characterize the nucleus replacement device in multiple mechanical bench tests, using ASTM-guided protocols, where appropriate. Mechanical bench testing included static testing to characterize the device's compressive, shear properties, and fatigue testing to determine the device's compressive fatigue strength, wear, and durability. Biomechanical testing, using human cadaveric lumbar spines, was also conducted to determine the ability of the device to restore multidirectional segmental flexibility and to determine its resulting endplate contact stress.

#### Results

The static compressive and shear moduli of the nucleus replacement device were determined to be between 4.2–5.6 MPa and 1.4–1.9 MPa, respectively. Similarly, the ultimate compressive and shear strength were 12,400 N and 6,993 N, respectively. The maximum axial compressive fatigue strength of the tested device that was able to withstand a runout without failure was determined to be approximately 3 MPa. The wear assessment determined that the device is durable and yielded minimal wear rates of 0.29mg/Mc. Finally, the biomechanical testing demonstrated that the device can restore the multidirectional segmental flexibility to a level seen in the intact condition while concurrently producing a uniform endplate contact stress.

#### Conclusions

The results of the present study provided a mechanical justification supporting the clinical use of the nucleus replacement device and also help explain and support the positive clinical results obtained from two European studies and one US pilot study.

#### Clinical Relevance

Nucleus replacement devices are rapidly emerging to address specific conditions of degenerative disc disease. Preclinical testing of such devices is paramount in order to potentially ensure successful clinical outcomes post implantation

**Key Words:** Nucleus replacement implant, lumbar intervertebral disc, biomechanics. *SAS Journal*. Winter 2008;2:28–39. DOI: SASJ-2007-0113-RR

### INTRODUCTION

Although the etiology and underlying pathology of low-back pain remains elusive, scientific investigations suggest that the loss of mechanical integrity and function of the intervertebral disc and its subsequent degeneration is a primary suspected cause.<sup>1</sup> Traditionally, the broad spectrum of low-back pain has been treated with either conservative nonoperative treatment or invasive surgical treatments such as spinal fusion. However, early restoration of the local anatomy and biomechanical function of a degenerated intervertebral disc may offer an appropriate first step to relieve pain and may delay the progression of adjacent

level disease. It is likely that with discogenic pain caused by mild to moderate disc degeneration, the annular and endplate mechanical integrity are not significantly or permanently compromised from mechanical overload. Hence, it is feasible to partially or completely restore the intradiscal annular and central endplate load transmission while restoring disc height and segmental kinematics.

Nucleus replacement technologies are re-emerging as treatment options aiming to restore the anatomy and the intradiscal load transmission patterns across a degenerative intervertebral disc.

Renewed interest in nuclear replacement has resulted from development of novel materials and technological innovations. Polyurethanes have been widely used for more than 40 years in implantable cardiovascular devices<sup>2</sup> but less commonly in orthopaedic devices.<sup>3</sup> Excellent durability, mechanical strength, and wear resistance, as well as chemical stability, are some of the reasons polyurethanes are being revisited in spinal implant development. Polyurethane has been shown to be useful as a biomaterial in a variety of spinal devices including posterior dynamic stabilization systems,<sup>4</sup> facet replacement systems,<sup>5</sup> disc replacement devices,<sup>6</sup> and even nucleus replacement devices.<sup>7</sup>

The DASCOR Disc Arthroplasty System (Figure 1A, Disc Dynamics, Inc., Eden Prairie, Minnesota) has recently been introduced as a nucleus replacement technology. The device consists of (1) a catheter-based polyurethane balloon of excellent cavity expansion and conforming capabilities; and (2) an in situ cured polyurethane core, optimized for resilience, flexibility, and mechanical strength. The device is fabricated by mixing a two-part, liquid, pre-polymer reactive system. This liquid mixture is then injected within a balloon placed in the prepared nucleotomy space (Figure 1B-C), using proprietary pressure parameters controlled by a custom injection system (Figure 2). The mechanical function of the balloon making it intrinsic to the device lies only within the implantation stage. The balloon's minimal thickness is designed to provide only a pressurized chamber for the liquid polyurethane to be injected and cured. Once the polyurethane core is cured, the expanded balloon adheres to the core and does not contribute to the device's resultant mechanical properties. The device's implantation method permits it to provide immediate disc height restoration<sup>8</sup> without relying on hydration, while providing a custom geometry that contours and conforms to any prepared nucleus cavity. This unique implantation feature ensures immediate axial and radial load transfer capabilities to the endplates and surrounding annulus.

The purpose of this study was to investigate the mechanical and biomechanical effectiveness of the DASCOR device. A series of mechanical bench and biomechanical tests were conducted as part of preclinical device characterization and performance testing.

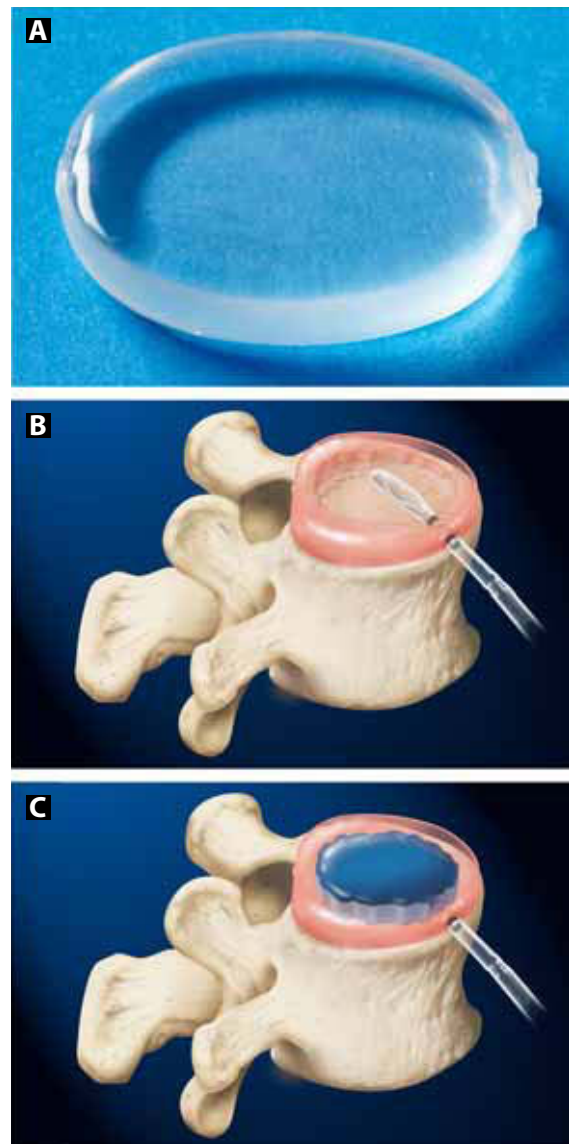
## MATERIALS AND METHODS

### Mechanical Bench Testing

#### *Overview of Sample Preparation and Testing Setup Methods*

All mechanical bench testing involved preparation of ellipsoid-shaped DASCOR samples of height and cross-sectional areas of approximately 10 mm and 450 mm<sup>2</sup>, respectively. Samples were soaked in saline for 21 days prior to any testing. A custom 6-station test fixture, mounted on a servo-pneumatic materials testing machine (Smart Test series SP 12600, Bose Corporation, Eden Prairie, Minnesota), was used to conduct all fatigue tests (Figure 3). During all testing the samples were immersed in a 37°C saline bath, without any radial constraining conditions

Figure 1.



The DASCOR device (A) is formed by inserting a balloon catheter into the prepared nucleotomy space (B) and injecting liquid polyurethane under pressure which cures in situ (C) within minutes to form the final device.

(ie, no simulated annulus), to create a worst-case sample test construct.

#### *Static Compressive and Shear Properties*

The static compressive properties were characterized in accordance to ASTM D575 and ASTM E111. Five DASCOR samples were tested using a typical servo-pneumatic materials testing machine (Smart Test series SP 12600). Axial compressive load was applied until sample failure. The load and displacement data of each tested sample was used to plot respective stress-strain curves, from which secant and tangent

Figure 2.



The software-controlled and tablet PC-monitored injection system used to implant the DASCOR device.

moduli at 5%, 10%, 15%, and 20% strain, as well as ultimate compressive strength, were computed.

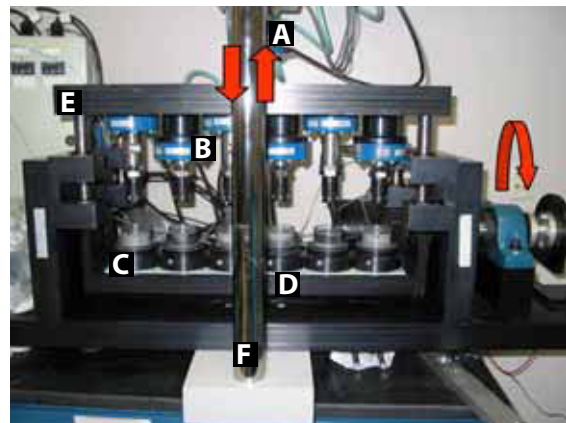
A shear modulus for each respective compression modulus was computed using the generalized Hooke's law of elasticity relationship<sup>9</sup> described for isotropic materials such as those used in the device. The ultimate shear strength of the device was characterized by testing 5 additional samples per ASTM D732.

### *Compressive Fatigue Strength*

The compressive fatigue strength of the tested nucleus replacement device was characterized in accordance to ASTM E466, ASTM E467, and ASTM E468. The purpose of this testing was to characterize the fatigue strength of the device using a destructive type of fatigue testing.

Twenty-one samples were tested in a series of constant amplitude axial compression loading tests, using a repeated stress cycle mode. The minimum cyclic axial compressive amplitudes were defined as 10% of the maximum cyclic loads examined (stress ratio (R) was 10). Cyclic loads were applied using a sinusoidal waveform pattern at a load frequency of 3 Hz. The series of cyclic tests were initiated by first subjecting sets of 3 samples to stress cycling at relatively large maximum load amplitude and then recording the number of cycles to failure. The procedure was then repeated on additional sets of

Figure 3.



The six-station custom wear testing apparatus used to conduct all the fatigue testing reported in this study. (A) The main load cell used to measure the total compressive load across all six stations. (B) The load cell used to measure the loads in each test station. (C) The bottom test station assembly used to mount a lower platen as well as the heater used to maintain test station fluids at 37°C. (D) The lower platform of the testing machine, which has the capability to rotate about its longitudinal axis. (E) The upper platform, which is attached to the actuator of the servo-pneumatic material testing machine. (F) The frame of the servo-pneumatic materials testing machine (Smart Test series SP 12600, Bose Corporation, Eden Prairie, Minnesota).

3 samples, at progressively decreasing load amplitudes, until a set of 3 samples were able to sustain a 10-million-cycle runout without failure.

Upon conclusion of all testing, the axial stress values versus the logarithm of the number of cycles to failure for each tested sample were plotted. A regression analysis using the method of least squares was used to obtain the best curve fit for an S-N plot. A mean axial compressive stress was calculated for each axial compressive load applied. The fatigue strength of the tested device was defined as the mean stress level at which no device failure occurred for a 10-million-cycle runout.

### *Mechanical Durability and Wear Assessment*

The durability and wear assessment of the nucleus replacement device was determined by loading 6 samples with a sinusoidal motion and loading waveform profile, simulating the intradiscal stress conditions during brisk walking.<sup>10-12</sup> Fatigue loading conditions consisted of  $\pm 5.5^\circ$  flexion/extension applied at 3 Hz, combined with axial compression ranging from 180 N (~0.4 MPa) to 520 N (~1 MPa), applied at 1.5 Hz. The motions and loads were synchronized so that peak axial compression occurred during peak flexion or extension, while the minimum axial compression occurred when the sample was in neutral position. These testing conditions resulted in the application of 10 million cycles of flexion/extension and 20 million cycles of axial compression. Three additional samples served as soaked controls, kept in 37°C saline and not subjected to load testing.



Prior to initiating the fatigue testing, and at multiple intervals throughout, both test and control samples were visually inspected and their mass, height, and compression modulus were also obtained. The saline fluid at each test station was also collected and replaced with fresh saline during each measurement interval. To determine sample durability, the mean sample compression modulus and height at initial, 5 million cycles, 10 million cycles, and recovery were statistically compared using a repeated measures analysis of variance. Durability was defined as the ability of samples to preserve their physical and compressive properties post wear assessment.

Wear assessment was computed in accordance to the methods described in ASTM 1714 and ASTM F2423. In brief, a regression analysis using the method of least squares was performed on the mass of soaked samples, enabling estimation of fluid absorption, so that the theoretical mass of test samples could be estimated. The total wear for each test sample, as well as a mean total, was estimated as the difference between the theoretical and actual sample mass measured. A mean wear rate was then computed from the resulting total wear.

All fluid samples collected during testing were sent to the Center for Clinical Bioengineering at the University of Texas Health Science Center at San Antonio for wear particle isolation and analysis. Using the descriptive wear particle morphology described in the ASTM F1877, the morphology of particles was determined. The 5 size and shape descriptors used to define each particle were (1) equivalent circle diameter; (2) roundness; (3) form factor; (4) aspect ratio; and (5) elongation factor. A repeated measures analysis of variance was used to statistically compare size and shape descriptors as a function of cycles.

## BIOMECHANICAL TESTING

Two non-destructive biomechanical studies using similar experimental methods were conducted on human lumbar cadaveric motion segments. The specific aims of these studies were to compare the (1) multidirectional flexibility of intact, nucleotomy, and nucleus replacement device constructs; (2) multidirectional flexibility of intact, water balloon, and nucleus replacement device constructs; and (3) endplate contact stress of water balloon and nucleus replacement device constructs during multidirectional flexibility testing.

Water balloon implants were constructed using a DASCOR balloon filled with water in an attempt to simulate the hydrostatic properties of a healthy nucleus pulposus.

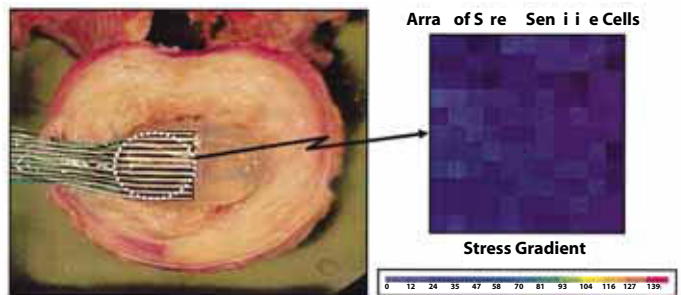
Four multisegmental human lumbar spines (T12 to L5; mean age  $54 \pm 7$  years) that had no history of spine pathology were used in these biomechanical studies. Twelve functional spinal units (FSUs: T12/L1, L2/3, L4/5) from these multisegmental spines were isolated and used for testing. The FSUs were divided into 2 groups of 6 and used for each multidirectional flexibility study. The experimental design of each study was similar and involved testing FSUs under the following conditions: (1) intact

(all 12 FSUs), (2) after nucleotomy ( $n=6$ ) or after a water balloon implant insertion ( $n=6$ ), and (3) after the nucleus replacement device implant insertion (all 12 FSUs).

The multidirectional flexibility testing was conducted using a servo-hydraulic materials testing machine (858 Mini-Bionix, MTS Corporation, Eden Prairie, Minnesota). The loads applied were axial compression, axial rotation, flexion/extension, and lateral bending. The maximum axial compressive load was 1200 N, while the maximum bending moment was 7.5 Nm. An axial compressive preload of 500 N was coupled with all bending conditions. Five load cycles were applied in each loading direction, with the fifth cycle used for data analysis.

All implants were inserted using a lateral approach. In 6 of the FSUs, a 0.1 mm thin, flexible stress transducer (K-Scan System,

**Figure 4.**



A typical example illustrating the placement of the stress sensor transducer (K-Scan System, Tekscan Inc, Boston, MA) between the DASCOR device and adjacent endplate (stress sensor is retracted backwards to show the device). Quantitative stress measurements are obtained from the array of sensing elements by assigning a color gradient with a small range of stress magnitudes. Stress uniformity is therefore measured by examining the variation of color gradients.

Tekscan Inc., Boston, Massachusetts) was inserted between the inferior endplate of the superior vertebra and the implant. This construct was used for FSUs that were implanted first with a water balloon implant and then with a DASCOR device (Figure 4).

The neutral zone (NZ), range of motion (ROM), and elastic stiffness were determined from all resulting load displacement curves obtained for each FSU construct condition, according to established methods.<sup>13</sup> Peak endplate contact stress levels for the water balloon and nucleus replacement device constructs were determined for each loading condition by averaging the results from the array of sensing elements at the maximum load. A repeated measures analysis of variance was used for each biomechanical study conducted to identify differences between FSU experimental conditions in NZ, ROM, stiffness, and peak endplate contact stress. Any significant differences were further evaluated through pairwise comparisons using Fisher's protected least significant difference method.

**RESULTS**

**Mechanical Bench Testing**

*Static Compressive and Shear Properties*

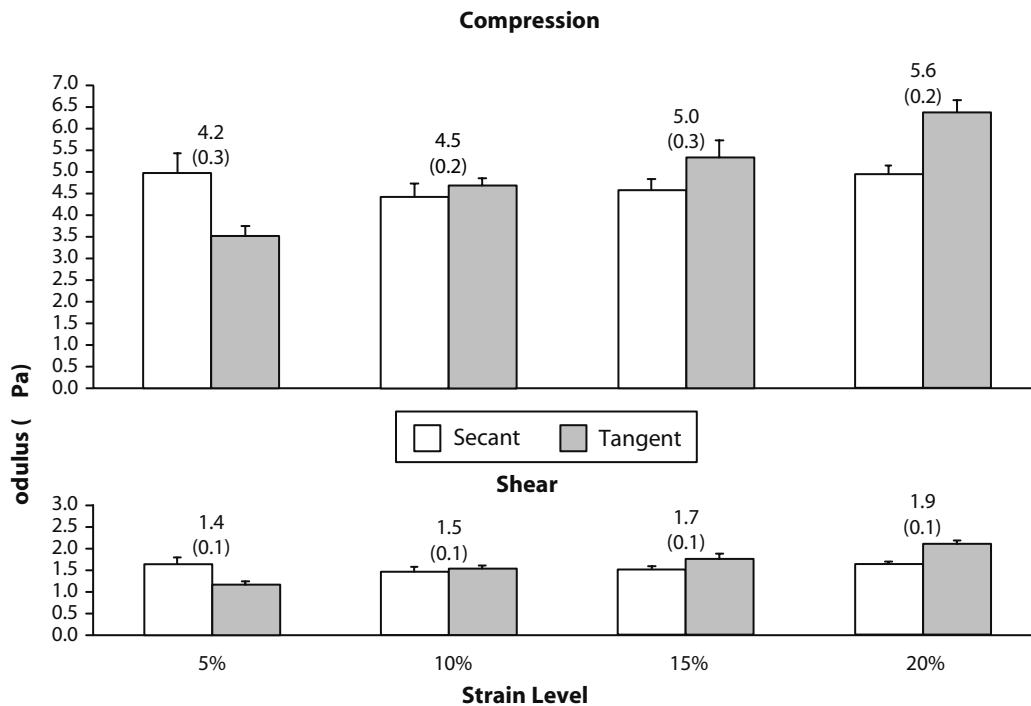
The mean secant compression and shear moduli at the reported strain levels were 4.7 MPa ± 0.3 MPa and 1.6 MPa ± 0.1 MPa, respectively (Figure 5). The mean tangent compression and shear modulus at the reported strain levels was 5.0 MPa ± 0.3 MPa and 1.7 MPa ± 0.1 MPa, respectively (Figure 5). The

able to withstand the 10-million-cycle runout was determined to be 2.94 MPa. The regression analysis demonstrated an excellent curve fit for the S/N plot with a correlation coefficient of 0.91, a coefficient of determination of 0.82, and a standard error of the estimate of 0.33 log-cycles.

**Mechanical Durability and Wear Assessment**

Generally, all samples tested experienced a significant progressive height loss ( $P < .0001$ ) directly related to the number

**Figure 5.** Compression and Shear Properties



Mean compression and shear moduli at different compressive strains obtained using the secant and tangent methods of modulus calculation. Values between bars denote the averaged value of modulus for a particular strain level. Values in parentheses and error bars denote one standard deviation.

overall compression modulus was determined to vary from 4.2 MPa ± 0.3 MPa to 5.6 MPa ± 0.2 MPa, while the respective shear modulus varied from 1.4 MPa ± 0.1 MPa to 1.9 MPa ± 0.1 MPa.

None of the samples failed at the maximal compressive load capabilities of the testing machine, and therefore the ultimate compressive strength of the DASCOR device could not be determined. However, the compressive strength of the sample at the maximum compressive load applied by the testing machine was 12,400 N or 25.7 MPa ± 0.7 MPa. Samples tested in shear had ultimate shear strength of 6,993 N ± 501 N or 8.0 MPa ± 0.6 MPa.

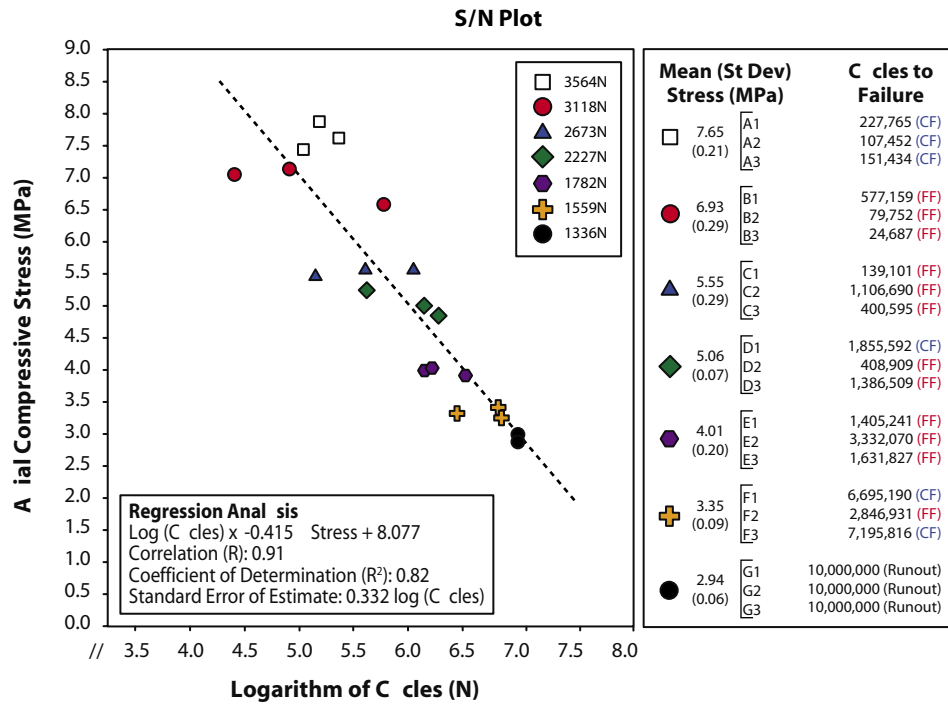
**Compressive Fatigue Strength**

The results of the testing are presented in Figure 6. The axial compressive fatigue strength of the nucleus replacement device

of cycles tested (Figure 7), that peaked to a mean height loss of 0.64 mm (6.4%) of initial height. However upon recovery, sample height returned within 0.17 mm (1.7%) of initial height. This recovered height (or permanent set) was not significantly different from initial height. The sample compression modulus significantly increased ( $P < .0001$ ) after 5 million cycles when compared to the sample's intact compression modulus (Figure 8) and remained constant until 10 million cycles of testing. The mean magnitude of compression modulus increase never exceeded 0.5 MPa throughout testing. Practically, the increase in compression modulus was not different from that measured in intact samples. Analysis of findings led to the conclusion that the nucleus replacement device samples successfully met durability criteria.

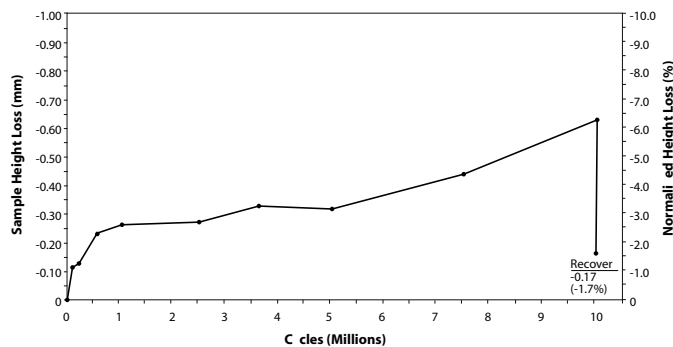
All samples completed the wear assessment without any gross morphological mechanical deterioration that could lead

Figure 6.



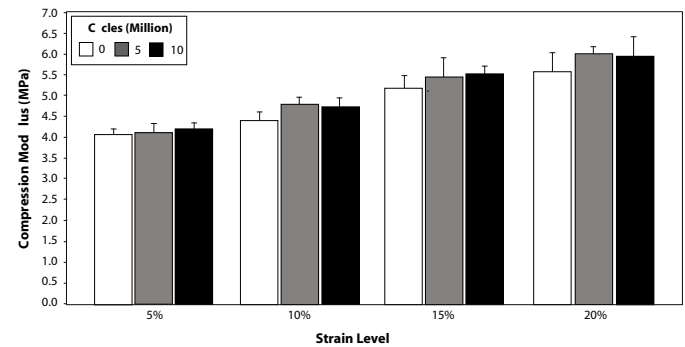
A plot of stress versus the number of cycles to failure (S/N) depicts the axial compressive fatigue strength of the DASCOR device (ie, ability to withstand 10 million cycles without failure). The mean axial compressive stress applied and the resulting number of cycles to failure for each tested sample is tabulated. The legend within the plot describes the axial compressive load (in newtons) of each sample tested.  
 Note: FF: Samples that experienced a functional failure, defined as the first appearance of a crack in the polyurethane core; CF: Samples that experienced a clinical failure, defined as the detachment of the balloon from the polyurethane core, without exhibiting the characteristics of a functional failure; Runout: Samples able to withstand 10 million cycles without failure.

Figure 7.



A plot illustrating the mean sample height loss (also normalized to intact height) experienced during the fatigue testing conducted to characterize the wear and durability of DASCOR samples. Residual height loss after sample recovery was defined as the permanent set.

Figure 8.

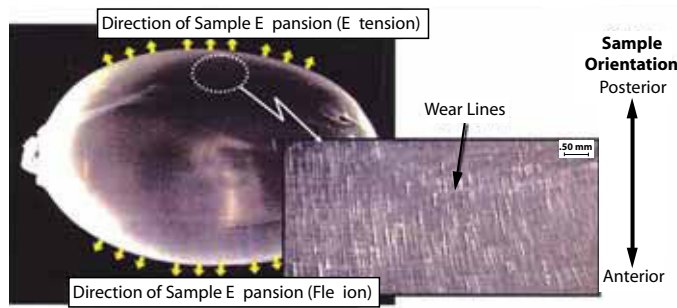


The mean compression modulus measured for DASCOR samples that underwent mechanical durability and wear assessment. Each compression modulus reported is a mean value obtained between the tangent and secant modulus measured for each strain level reported.

to failure. Minimal surface abrasions, pitting and wear line formation were observed along the distal periphery of the sample (notably along the most anterior and posterior sample edges), in areas where the combined axial and bending stress on the sample was the highest (Figure 9). Mean total wear stress across all samples tested was 2.92 mg (0.067% of the mean initial sample mass) (Figure 10). The mean predicted wear rate was determined to be 0.29 mg per million cycles (0.007% of the mean intact mass per million cycles).

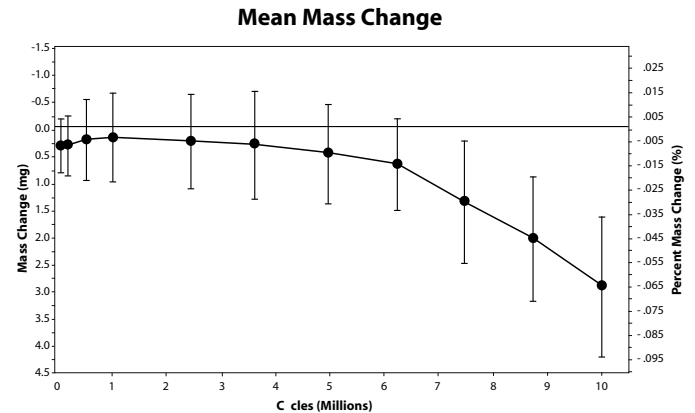
The morphology of particles observed was primarily rough spherical, spheroidal, or agglomerated globular (Table 1). Very few rough and irregular flakes were seen. On average, most of the particles were larger than 1 µm in diameter with a distribution of

Figure 9.



A depiction of the wear location that occurred on the DASCOR balloon on samples tested for mechanical durability and wear assessment. The small yellow arrows denote the direction of the sample's maximal radial expansion during cyclic flexion and extension movements. A magnified view of the peripheral sample area most radial with respect to the center of the DASCOR samples showed evidence of minor wear line scratches, minor pitting, and deposition of wear particles, all consistent with the direction of radial expansion during wear testing. The latter sample location also experienced the highest total stress when compared to central sample locations (ie, bending stresses were highest most distally to the major diameter and nearly zero along the major diameter).

Figure 10.



A plot of the mean mass change versus the number of flexion/extension cycles for all DASCOR samples that underwent mechanical durability and wear assessment. The y axis on the right also provides a scale which normalizes the mass change as a function of the mean initial sample mass. Error bars reflect one standard deviation.

particles extending up to 19 µm in diameter. With an increasing number of cycles, the proportion of globular and flake particles significantly decreased while the proportion of spherical or spheroidal particles significantly increased ( $P < .05$ ). Similarly, particles appeared to become rounder and smoother with an increasing number of cycles (Figure 11).

**Biomechanical Testing**

None of the implants extruded during either series of flexibility testing.

**Intact Versus Nucleotomy Versus Nucleus Replacement Constructs**

A significant difference was found for the overall NZ measured across the 3 experimental conditions ( $P = .0076$ ; Figure 12). The NZ of the nucleotomy construct increased compared to the intact construct. Implantation of the nucleus replacement device

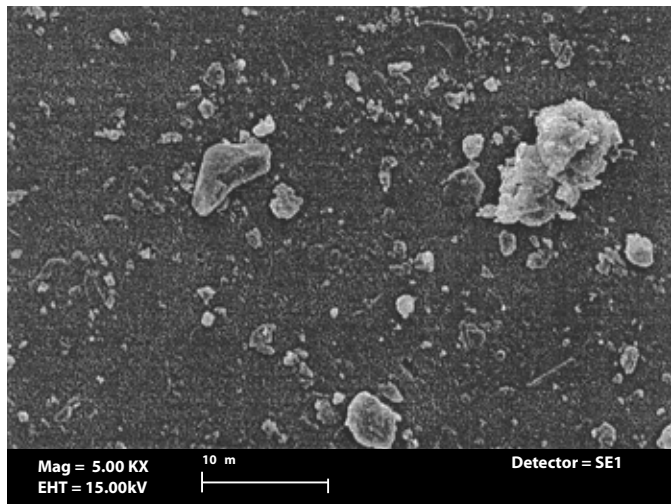
Table 1.

Particle Shape Descriptor	Cycles (Millions)						
	0	0.5	2.5	5	6.25	7.5†	10†
Equivalent Circle Diameter(µm)	1.22 (0.74)	1.34 (0.92)	1.55 (1.51)	1.36 (0.89)	1.17 (1.21)	1.69 (3.62)	1.04 (1.75)
Aspect Ratio	1.45 (0.32)	1.45 (0.34)	1.54 (0.46)	1.51 (0.43)	1.42 (0.45)	1.33 (0.22)	1.35 (0.26)
Elongation	1.74 (0.61)	1.73 (0.63)	1.93 (0.81)	1.85 (0.88)	1.63 (0.78)	1.51 (0.45)	1.51 (0.51)
Roundness	0.74 (0.13)	0.75 (0.13)	0.71 (0.15)	0.72 (0.14)	0.82 (0.16)	0.83 (0.13)	0.83 (0.13)
Form Factor	0.88 (0.07)	0.88 (0.08)	0.85 (0.10)	0.87 (0.09)	0.92 (0.09)	0.93 (0.07)	0.93 (0.08)

Mean particle shape characteristics as defined by ASTM F1877 using SEM visual inspection. Particle shape descriptors in cycle time points denoted with an "†" were significantly different than the rest ( $P < .05$ ). Values in parentheses denote one standard deviation.



Figure 11.



A scanning electron micrograph of typical particles observed in sample solutions used for particle characterization.

significantly restored the NZ, regardless of loading direction, to those measured for intact constructs.

A significant difference was found for the overall ROM measured across the 3 experimental conditions ( $P < .0001$ ; Figure 12). The ROM of the nucleotomy construct increased compared to the intact construct, with significant increases in compression, in axial rotation and flexion/extension. The ROM of the nucleotomy construct during lateral bending was not significantly different than the ROM of the intact condition. Implantation of the nucleus replacement device significantly restored the ROM, regardless of loading direction, back to within  $\pm 4\%$  of the ROM observed for intact constructs.

A significant difference was found for the stiffness measured across the 3 experimental conditions ( $P < .0001$ ; Figure 12). A significantly increased stiffness ( $P < .0001$ ) was observed for the nucleotomy condition when compared to the intact condition, during flexion/extension and lateral bending. Conversely, the stiffness in the nucleotomy condition was decreased compared to the intact construct during compression and axial rotation. Implantation of the nucleus replacement device significantly restored the segmental stiffness, regardless of loading direction, to that observed for the intact construct.

**Intact Versus Water Balloon Versus Nucleus Replacement Device Constructs**

No significant difference was found in the overall NZ and ROM measured in the intact, water balloon, and nucleus replacement device constructs, regardless of loading direction (Figure 13). The water balloon construct demonstrated a marginally significant trend of decreased stiffness ( $P = .0778$ ; Figure 13) when compared to both the intact and nucleus replacement device constructs. This decrease in stiffness was greatest during

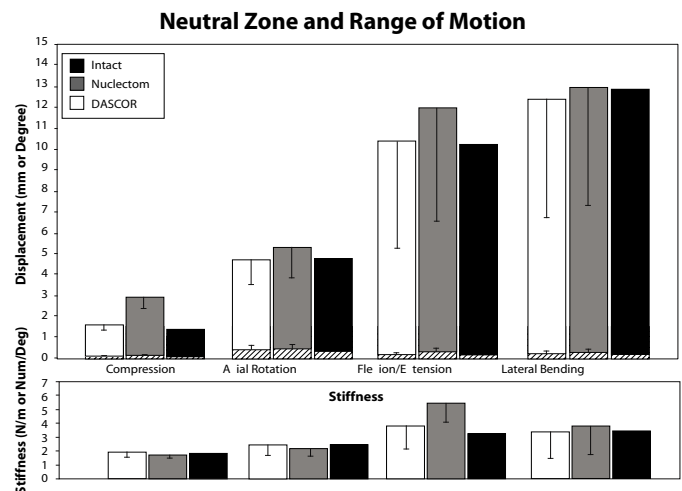
flexion/extension. Implantation of the device restored stiffness to that observed for intact constructs.

A significant difference was found in peak endplate contact stress measured with the water balloon and nucleus replacement device constructs (Table 2) during peak compressive or bending loads ( $P = .0002$ ). Although statistically significant, the difference in peak endplate contact stress between the water balloon and nucleus replacement device constructs was never greater than 0.10 MPa to 0.16 MPa. Practically, this relative change in stress is considered insignificant.

**DISCUSSION**

The purpose of this study was to assess the DASCOR device in order to provide a preclinical mechanical or biomechanical evaluation and physiological justification for its use. The methods used mechanically characterized the device in an unconfined setup (ie, without a simulated annulus) using

Figure 12.

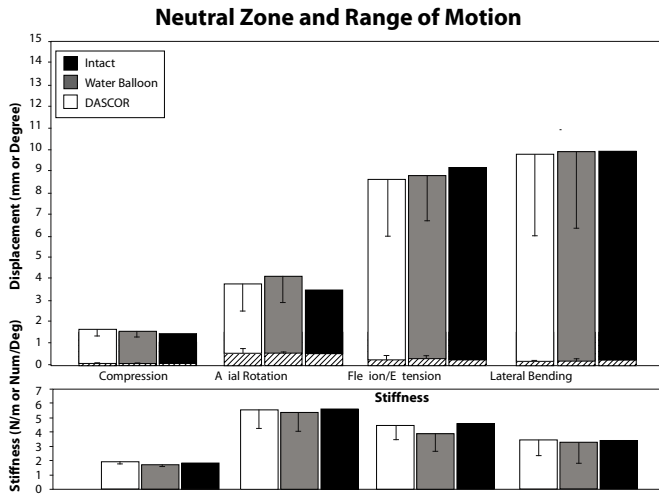


A figure depicting the multidirectional flexibility results comparing the intact, nucleotomy, and nucleus replacement device segmental constructs. The graph on top presents the results obtained for neutral zone (crossed line bars within solid shaded bars) and range of motion. The bottom graph presents results obtained for segmental stiffness. Error bars reflect one standard deviation.

clinically relevant device sizes as confirmed retrospectively from sizes of devices implanted in ongoing clinical studies.<sup>8</sup> It is important to note that these tests were conducted when relevant ASTM recommendations were unavailable. Therefore, testing such as the wear characterization reported in this study should be understood as offering a preliminary wear evaluation of the device, since not all loading directions were assessed. The effects of device migration and extrusion were not examined in the present study. Finally, implant extrusion did not occur during the biomechanical testing conducted in this study.

The principal functions of any nucleus replacement implant are to alleviate pain in a pathological lumbar spine segment

Figure 13.



A figure depicting the multidirectional flexibility results comparing the intact, water balloon and nucleus replacement device segmental constructs. The graph on top presents the results obtained for neutral zone (crossed line bars within solid shaded bars) and range of motion. The bottom graph presents results obtained for segmental stiffness. Error bars reflect one standard deviation.

through removal of painful pro-inflammatory disc tissues while preserving or restoring (1) segmental flexibility and stability; (2) anatomical disc height during activities of daily living; and (3) some load transmission capacity across the motion segment and within the anterior column, in order to interrupt, ideally arrest, or delay the degenerative cascade of motion segment tissues. Both the present study and previous investigations<sup>14,15</sup> suggest that there are four main mechanical characteristics in a nucleus replacement device that could dictate, along with their interplay, if these functions can be satisfied: (1) the ability to conform to a nucleus cavity; (2) the material properties such as compression modulus; (3) the ability to permit segmental flexibility with preservation of disc height; and (4) the ability to minimize or eliminate migration.

An advantage during the implantation stage of the DASCOR device is the ability to pressurize the contained balloon environment and as a result fill any given cavity created during nucleotomy. The ability to conform to a nucleus cavity is important and ensures that uniform axial, radial, and circumferential load transmission occurs across the endplates or annulus, ensuring that inward annular bulging is avoided. Inward annular bulging, typically present with degeneration of the nucleus pulposus,<sup>16,17</sup> can lead to annular delamination, which further worsens annular degeneration. Experimental<sup>15</sup> and finite element<sup>14</sup> studies have demonstrated that if a nucleus replacement device maintains intimate contact with the surrounding annulus, inward annular bulging can be avoided.

The flexibility testing in this study showed no significant differences between the water balloon and nucleus replacement device constructs for the parameters measured, except for

Table 2.

Loading Condition	Contact Stress (MPa)		
	Water Balloon	DASCOR®	Difference
Compression	0.94 (0.19)	0.80 (0.06)	<i>0.16</i> (0.19)
Axial Rotation	0.32 (0.09)	0.21 (0.02)	<i>0.10</i> (0.08)
Flexion	0.71 (0.28)	0.56 (0.14)	<i>0.10</i> (0.16)
Extension	0.51 (0.23)	0.44 (0.08)	<i>0.12</i> (0.16)
Lateral Bending	0.49 (0.26)	0.39 (0.09)	<i>0.15</i> (0.15)

The mean contact stress measured at the interface between the implant and the lower endplate during multi-directional segmental flexibility testing. The mean difference in contact stress between the two implant constructs tested is denoted in italics. Values in parentheses denote one standard deviation.

endplate contact stress (difference between constructs was 0.10–0.16 MPa). A common misconception is that the compression modulus of a nucleus replacement device should be similar to that of a healthy nucleus pulposus. The presumed rationale is that complete intradiscal axial, circumferential, and radial load transmission would be restored across the annulus and endplates. It is presumed that such nucleus implants would restore segmental stability, through implant deformations that would preserve, during daily activities, a clinically relevant disc height necessary to avoid impingement of neural structures.

Nucleus replacement devices of a compression modulus simulating a healthy nucleus pulposus may redistribute the central axial stress to more circumferential and radial stress, thus increasing the demands on the annulus. This includes devices simulating the nucleus hydrostatic conditions or with a compression modulus less than 1 MPa. However, in a clinical situation considered appropriate for a nucleus replacement procedure, the annulus has suffered degenerative changes such as those described by fissures, clefts, tears, and delaminations.<sup>18</sup> The iatrogenic annular damage caused by implantation disrupts the annular integrity further. These effects suggest that the annulus may not be competent enough to afford a complete restoration of load transmission as is possible in its healthy state. Furthermore, a nucleus device of a low compression modulus may provide excessive axial deformations during daily activities that exceed the critical disc height needed to avoid neural impingement. In such conditions, the axial load transmission across the lumbar motion segment would also be shifted more posteriorly, predisposing the facet joints and posterior annulus to increased localized stress<sup>19</sup> and strain.<sup>17</sup> Consequently, the attempt to re-establish load transmission, disc height, and segmental stability may lead to further motion segment failure and recurrence of low-back pain.

High compression modulus exhibited by devices with a compression modulus similar to bone<sup>20</sup> or greater,<sup>21</sup> as well

as articulating nucleus devices,<sup>22</sup> reduce circumferential and radial stress to the annulus but impose greater endplate axial compressive stress. These devices may initially preserve a critical disc height and restore segmental stability by not causing any axial deformations and relying on either the endplates to glide over the implant's bearing surfaces or the articulation provided within the implant. However, central vertebral or endplate locations adjacent to a degenerative nucleus pulposus are known to experience less loading due to the loss of nucleus hydrostatic pressure.<sup>23</sup> These sites have remodeled the underlying bone according to Wolff's Law<sup>24</sup> (ie, weakened vertebral strength due to decreased bone density<sup>25</sup>). Furthermore, the inflammatory reaction due to the nucleotomy procedure also aggravates the endplate integrity by increasing endplate marrow changes (ie, Modic changes).<sup>26</sup> It is likely that the rate of vertebral bone remodeling to accommodate a new increased central axial stress environment due to nucleus device implantation may be limiting and may result in subsidence. Previous scientific investigations have demonstrated a higher risk of nucleus implant subsidence<sup>21,27</sup> that is believed to be associated with a high compression modulus that increases localized central axial stress.

Previous bench studies have characterized the DASCOR device as an isotropic, incompressible material. The results of this study determined the compression modulus of the device to be between 4.2 MPa and 5.6 MPa. The compression modulus did not appear to significantly change or be influenced by wear and permanent set and was sufficient to restore the multidirectional flexibility to that observed in an intact lumbar motion segment. Furthermore, a uniform endplate contact stress was obtained by segments implanted with the nucleus replacement device, which were not practically different than those experienced by a hydrostatic pressurized implant simulated by the water balloon implant. It appears that the compression modulus of the device allowed segmental stability to be achieved through a combination of axial deformation that preserved disc height and gliding of endplates over the implant's bearing surfaces.

Meakin et al.<sup>14</sup> determined in a finite element model that the optimal compression modulus for a nucleus replacement device should be roughly 3 MPa. These findings were based on the ability of the device to restore annular stress to those levels seen in a healthy annulus with isotropic material properties. This characteristic represents a limitation of their study because healthy intervertebral discs do not represent the clinical indication for nucleus replacement surgery. Nonetheless, their results do suggest that a compression modulus higher than 3 MPa (such as that of the DASCOR device) may be suitable for the degenerated annulus commonly encountered in clinical indications requiring nucleus replacement. The clinical experience of the DASCOR device, which includes over 100 patients worldwide and extends to over 2 years of follow-up,<sup>8</sup> has not revealed endplate subsidence or annular failure. Therefore, these results provide preliminary evidence that the compression modulus of this device does not pose significant risks and is well suited for its intended use.

The static compressive and shear strength of the nucleus replacement device was determined to be 11,649 N (25.7 MPa) and 6,993 N (8 MPa), respectively. The device demonstrated a mechanical strength that is well beyond the ultimate strength of the lumbar spine in either compressive<sup>25,28</sup> or shear<sup>29</sup> loading. Furthermore, the axial compressive fatigue strength of the DASCOR device was approximately 3 MPa (direct cyclic axial loading on the device), corresponding to high physiological loads as measured by Nachemson et al.<sup>30,31</sup> The axial fatigue strength measured for the DASCOR device is highly unlikely to occur, in the same repetitive frequency, in a person's activities of daily living. The majority of intradiscal pressures corresponding to activities of daily living are typically in the order of 0.6–1.6 MPa.<sup>30-32</sup>

The preliminary wear assessment of the DASCOR device was in the same range of physiological loading as that reported in the literature and demonstrated total wear and wear rates of 2.92 mg and 0.29 mg/Mc, respectively. The wear rates obtained in this study are similar to wear rates reported for the NeuDisc<sup>33</sup> (0.25 mg/Mc) (Replication Medical, Inc., New Brunswick, New Jersey) and NUBAC<sup>22</sup> (0.28 mg/Mc) (Pioneer Surgical Technology, Marquette, Michigan) nucleus replacement implants. The wear rates reported for the BRYAN Cervical Disc<sup>6</sup> (Medtronic Sofamor Danek, Memphis, Tennessee), a cervical total disc replacement implant with a polyurethane component, are in the order of 1.2 mg/Mc. These wear rates are four times higher than those of the DASCOR device. The wear rates obtained for the DASCOR device are expected to have a minimal risk of osteolysis, based on historical data from hip replacements,<sup>34</sup> but also from an in vivo baboon biodurability study conducted on the DASCOR device.<sup>35</sup>

The number of wear particles generated from the wear testing of this study was qualitatively judged to be less than those observed for ultra high molecular weight polyethylene (UHMWPE)<sup>36</sup> wear particles retrieved from human tissue. Furthermore, particles obtained from the wear assessment were almost twice the size of similar UHMWPE particles retrieved from failed hip replacements.<sup>36</sup> The inflammatory response of DASCOR wear debris has been studied in the rabbit model, and the results have shown that the DASCOR wear particles caused no significant biological response.<sup>37</sup>

In conclusion, the results of the present study provided a preclinical mechanical justification supporting the clinical use of the DASCOR device and also help explain and support the positive clinical results obtained from two European<sup>8</sup> studies and one US pilot study.

---

Anthony Tsantrizos, MSc, PhD, Nathaniel R. Ordway, MS, PE, Khin Myint, Erik Martz, MSc; Hansen A. Yuan, MD

From Disc Dynamics, Inc., Eden Prairie, Minnesota (Tsantrizos, Myint, and Martz); Department of Orthopaedic Surgery, SUNY Upstate Medical University, Syracuse, New York (Ordway and Yuan)



Anthony Tsantrizos, Khin Myint, and Erik Martz are employees of Disc Dynamics, Inc., the manufacturer of the device used in this study.

Address correspondence to Anthony Tsantrizos, Disc Dynamics, Inc., 9600 West 76th Street, Suite T, Eden Prairie, Minnesota, 55344 (email: atsantrizos@discdyn.com)

This manuscript was submitted August 30, 2007, and accepted for publication November 28, 2007.

The authors would like to thank Robert Kohler, Dan Melink, Qi-Bin Bao, PhD, Robert Garryl Hudgins, PhD, Frederick Werner, and Mauli Agrawal, PhD, PE, for their valuable assistance.

Financial support for this study was provided by Disc Dynamics, Inc.

## REFERENCES

1. Luoma K, Riihimaki H, Luukkonen R, Raininko R, Viikari-Juntura E, Lamminen A. Low back pain in relation to lumbar disc degeneration. *Spine*. 2000;25(4):487-492.
2. Bruck SD. Medical applications of polymeric materials. *Med Prog Technol*. 1982;9(1):1-16.
3. Mandarino MP, Salvatore JE. Polyurethane polymer (ostamer): its use in fractured and diseased bones; experimental results. *Surg Forum*. 1958;9:762-765.
4. Stoll TM, Dubois G, Schwarzenbach O. The dynamic neutralization system for the spine: a multi-center study of a novel non-fusion system. *Eur Spine J*. 2002;11:S170-178.
5. Wilke HJ, Schmidt H, Werner K, Schmolz W, Drumm J. Biomechanical evaluation of a new total posterior-element replacement system. *Spine*. 2006;31(24):2790-2796.
6. Anderson PA, Rouleau JP, Bryan VE, Carlson CS. Wear analysis of the Bryan Cervical Disc prosthesis. *Spine*. 2003;28(20):S186-194.
7. Korge A, Nydegger T, Polard JL, Mayer HM, Husson JL. A spiral implant as nucleus prosthesis in the lumbar spine. *Eur Spine J*. 2002;11:S149-153.
8. Ahrens M, Donkersloot P, Martens F, et al. Nucleus replacement with the DASCORTM Disc Arthroplasty System: Two year follow up results obtained from two prospective European multi-center clinical studies. Paper presented at: Spine Arthroplasty Society; May 1-4, 2007; Berlin, Germany.
9. Beer FP, Johnston ER. *Mechanics of Materials*. 2nd ed. London: McGraw-Hill Book Company; 1992.
10. Callaghan JP, Patla AE, McGill SM. Low back three-dimensional joint forces, kinematics, and kinetics during walking. *Clin Biomech*. 1999;14(3):203-216.
11. Nachemson A, Elfstrom G. Intravital dynamic pressure measurements in lumbar discs. A study of common movements, maneuvers and exercises. *Scand J Rehabil Med*. 1970;1S:1-40.
12. Syczewska M, Oberg T, Karlsson D. Segmental movements of the spine during treadmill walking with normal speed. *Clin Biomech*. 1999;14(6):384-388.
13. Panjabi MM. The stabilizing system of the spine. Part II. Neutral zone and instability hypothesis. *J Spinal Disord*. 1992;5(4):390-396.
14. Meakin JR, Hukins DW. Replacing the nucleus pulposus of the intervertebral disk: prediction of suitable properties of a replacement material using finite element analysis. *J Mater Sci*. 2001;12:207-213.
15. Meakin JR, Reid JE, Hukins DW. Replacing the nucleus pulposus of the intervertebral disc. *Clin Biomech*. 2001;16(7):560-565.
16. Seroussi RE, Krag MH, Muller DL, Pope MH. Internal deformations of intact and denucleated human lumbar discs subjected to compression, flexion, and extension loads. *J Orthop Res*. 1989;7(1):122-131.
17. Tsantrizos A, Ito K, Aebi M, Steffen T. Internal strains in healthy and degenerated lumbar intervertebral discs. *Spine*. 2005;30(19):2129-2137.
18. Farfan HF, Huberdeau RM, Dubow HI. Lumbar intervertebral disc degeneration: the influence of geometrical features on the pattern of disc degeneration—a post mortem study. *J Bone Joint Surg*. 1972;54A(3):492-510.
19. Adams MA, McNally DS, Dolan P. 'Stress' distributions inside intervertebral discs. The effects of age and degeneration. *J Bone Joint Surg*. 1996;78B(6):965-972.
20. Cook S, Salkeld S, Rogozinski A, Rogozinski C, Bailey K. Partial disc replacement in the baboon lumbar spine. Paper presented at: Spine Arthroplasty Society; May 9-13, 2006; Montreal, Quebec, Canada.
21. Fernstrom U. Arthroplasty with intercorporeal endoprosthesis in herniated disc and in painful disc. *Acta Chir Scand Suppl*. 1966;357:S154-159.
22. Bao QB, Songer M, Pimenta L, et al. NUBACTM Intradiscal Arthroplasty: Preclinical studies, and preliminary safety and efficacy evaluations. *SAS J*. 2007;1(1):36-46.
23. Roberts S, McCall IW, Menage J, Haddaway MJ, Eisenstein SM. Does the thickness of the vertebral subchondral bone reflect the composition of the intervertebral disc? *Eur Spine J*. 1997;6(6):385-389.
24. Wolff JD. Das gesetz der tranformation der knochen. *Berlin Hirschwald*. 1892.
25. Hansson T, Roos B, Nachemson A. The bone mineral content and ultimate compressive strength of lumbar vertebrae. *Spine*. 1980;5(1):46-55.
26. Crock HV. Internal disc disruption. A challenge to disc prolapse fifty years on. *Spine*. 1986;11(6):650-653.
27. Schoenmayer R. Ten year follow-up of disc height, range of motion and clinical outcomes with 1st generation PDN device. Paper presented at: Spine Arthroplasty Society; May 9-13, 2006; Montreal, Quebec, Canada.
28. Genaidy AM, Waly SM, Khalil TM, Hidalgo J. Spinal compression tolerance limits for the design of manual material handling operations in the workplace. *Ergonomics*. 1993;36(4):415-434.
29. Cripton P, Berleman H, Visarius H, Begeman PC, Nolte LP, Prasad P. Response of the lumbar spine due to shear loads. Paper presented at: Symposium: Injury prevention through biomechanics, 1995; Wayne State University, Detroit MI.
30. Nachemson A. The effect of forward leaning on lumbar intradiscal pressure. *Acta Orthop Scand*. 1965;35:314-328.
31. Nachemson A. In vivo discometry in lumbar discs with irregular nucleograms. Some differences in stress distribution between normal and moderately degenerated discs. *Acta Orthop Scand*. 1965;36(4):418-434.
32. Nachemson AL, Morris J. In vivo measurements of intradiscal pressure. *J Bone Joint Surg*. 1964;46A:1077-1092.
33. Bertagnoli R, Prewett A, Yue JJ, Sabatino C. Chapter 16 - NeuDisc. In: Kim DH, Cammisa FP, Fessler RG, eds. *Dynamic Reconstruction of the Spine*. New York: Thieme Medical Publishers inc.; 2006:122-127.

34. Dumbleton JH, Manley MT, Edidin AA. A literature review of the association between wear rate and osteolysis in total hip arthroplasty. *J Arthroplasty*. 2002;17(5):649-661.
35. Cunningham B, Hu N, Beatson HJ, McAfee P, Yuan HA. An investigational study of nucleus pulposus replacement using an in-situ curable polyurethane. An in vivo non-human primate model. Paper presented at: Spine Arthroplasty Society; May 1-4, 2007; Berlin, Germany.
36. Mabrey JD, Afsar-Keshmiri A, Engh GA, et al. Standardized analysis of UHMWPE wear particles from failed total joint arthroplasties. *J Biomed Mater Res*. 2002;63(5):475-483.
37. Lacy S, Johnson C, Long PH, et al. A Rabbit Model to Evaluate the Biological Response to DASCOR™ Device Wear Debris. Paper presented at: Spine Arthroplasty Society; May 1-4, 2007; Berlin, Germany.